Available online at www.sciencedirect.com
SCIENCE DIRECT®
Carbohydrate Research 339 (2004) 123–131
Carbohydrate RESEARCH

Arabinan–cellulose composite in *Opuntia ficus-indica* prickly pear spines

M. R. Vignon,[a,*] L. Heux,[a] M.-E. Malainine[a,b] and M. Mahrouz[b]

[a]*Centre de Recherches sur les Macromolécules Végétales (CERMAV-CNRS), Université Joseph Fourier, BP 53, 38041 Grenoble Cedex 9, France*
[b]*Unité de Chimie Agroalimentaire, Laboratoire de Chimie Organique Appliquée, Département de Chimie, Faculté des Sciences Semlalia, Université Cadi Ayyad, BP 2390, 40001 Marrakech, Morocco*

Received 30 May 2003; revised 17 September 2003; accepted 22 September 2003

Abstract—The ultrastructure of the spines decorating the cladodes of the cactus *Opuntia ficus-indica* was investigated by optical microscopy, scanning and transmission electron microscopy, wide angle X-ray, and solid state ^{13}C NMR analyses. Each spine consisted of a compact parallel arrangement of slender cellulosic fibers (0.4 mm in length and 6–10 μm in diameter) with small lumens. The fibers were disencrusted by alkali and sodium chlorite bleaching, yielding a remarkable arabinan–cellulose (1:1) product. X-ray fiber diagrams of the spines before and after purification confirmed the presence of crystalline cellulose domains with molecular axis parallel to the spine axis. CP-MAS ^{13}C $T1$ NMR data showed a strong interaction at a nanometric level of a fraction of the arabinan and the cellulose crystalline domains. By sequential hydrothermal extractions, followed by a trifluoroacetic acid treatment, a relatively pure cellulose was isolated while the extracted fibers became fibrillated into slender microfibrils having no more than 4–6 nm diameter. The hydrothermal extract yielded the α-L-arabinofuranan consisting of a chain of $(1\rightarrow5)$-linked L-arabinosyl residues with branching either at C-2 or C-3 or at both C-2 and C-3. Taken together, these observations suggest that the bulk of the spine fibers consists of an intimate composite of cellulose microfibrils embedded in an arabinan matrix.

Keywords: Cactus spine; *Opuntia ficus-indica*; Microscopy; Ultrastructure; Cellulose; Arabinan; ^{13}C CP-MAS NMR

1. Introduction

Cactus pear *Opuntia ficus-indica* (OFI) originated from the American continent and reached the Mediterranean countries during the 16th century. Cactus pear is mainly cultivated for fruit production.[1] Young shoots are also eaten as vegetables (Napolitos) in Mexico and southern USA. In North Africa, the cultivation of OFI is used on the one hand against the soil erosion in arid areas, and on the other as forage replacement during droughts. There is a growing interest in the nonfood usage of OFI, mainly in medical applications, as ethanol extracts of OFI have been shown to have potential analgesic and anti-inflammatory effects.[2] Ingestion of raw and cooked OFI extracts has beneficial effects on levels of cholesterol without secondary effect on amounts of glucose and lipoproteins in blood.[3]

Cellulose is the structural polymer that confers mechanical properties to all higher plant cells where it is usually found in the form of microfibrils that are themselves organized in fibers, cell walls, etc. In the cellulose microfibrils, the cellulose chains are rigorously aligned parallel to the microfibril axis. This perfect organization confers to the microfibril mechanical properties that are close to the theoretical limit for cellulose. The cactus spines have a remarkable stiffness, which is probably related to their defensive role. It is believed that this stiffness is due to the organization of the cellulose within the spines.

In a previous work we showed that in our OFI samples the spines corresponded to about 8.4 wt% on a

* Corresponding author. Tel.: +33-476-03-76-14; fax: +33-476-54-72-03; e-mail: vignon@cermav.cnrs.fr

0008-6215/$ - see front matter © 2003 Elsevier Ltd. All rights reserved.
doi:10.1016/j.carres.2003.09.023

dry weight basis of the whole cladodes.[4] OFI spines consisted of 96% of polysaccharides with approximately equal amounts of cellulose and arabinan.

L-Arabinose containing polysaccharides was found in different plant families, in the cell walls of roots,[5–7] bark,[8,9] trunks,[10,11] seeds,[12–14] fruits,[15] in primary cell walls,[16–19] or in the cortex cell walls of hemp and flax.[20,21] Arabinans are usually constituted of poly-α-(1 → 5) arabinofuranosyl chains, and are generally associated with pectic substances, as lateral chains in the hairy regions of pectins. This classical configuration confers a rather complex and heavily branched structure to arabinose containing polysaccharides.

Following a preliminary report,[4] the goal of this paper was to correlate the ultrastructure and chemical composition of the spines from cactus OFI, in order to get a better knowledge of the organization of the unusual L-arabinan–cellulose composite occurring in the spine fibers. A first step of the study involved the extraction and chemical analysis of the arabinan. The resulting data were used in a CP-MAS solid state ^{13}C NMR spectroscopy study to analyze the structural organization of the cellulose–arabinan complex constituting the bulk of the spines.

2. Experimental

2.1. Materials and analytical methods

Fresh cladodes were collected in Amezmiz (Morocco); the spines were removed manually from cladodes. The neutral sugars, uronic acid, minerals, fats, waxes, and lignin analysis were determined according to a procedure already described[4]. The methylation analysis of the arabinan fraction was achieved according to the procedure of Sanford and Conrad,[22] followed by TFA hydrolysis, conversion of the monomers into methylated alditol acetates identified by GLC–MS.

2.2. Purification

2.2.1. Alkali extraction/sodium chlorite bleaching. The different steps of the purification process are presented in Figure 1. The spines (25 g), after elimination of fats and waxes, were suspended in 500 mL 0.5 M NaOH solution, shaken for 2 h at 80 °C, filtered and washed with water. After a second extraction under the same conditions, the alkali-insoluble product was recovered on a 60 μm sieve, washed extensively, and then bleached with $NaClO_2$.

2.2.2. Hydrothermal extraction of arabinan. The purified fibers (0.5 g) were inserted into a 100 mL steel autoclave filled with 60 mL 0.125 M NaOH. The autoclave was sealed and brought to 180 °C in an oil bath. After 1 h at this temperature, it was cooled under running tap water and the fibers were recovered by pressure filtration. The solid residue was washed with distilled water, and subjected to two more hydrothermal extractions and filtration steps. The resulting three filtrates (arabinan **1**, **2**, **3**) were pooled, neutralized to pH 7.0, and freeze-dried for further analysis.

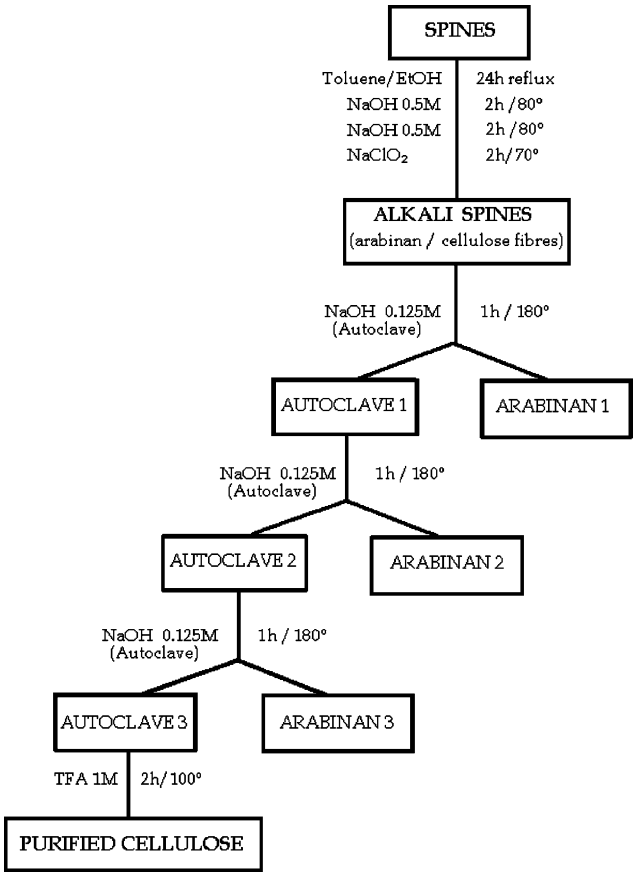

Figure 1. Fractionation scheme of the OFI spines.

2.2.3. TFA treatment. The resulting purified sample was finally treated with 1 M TFA for 2 h at 100 °C. The filtrate was removed, the residue washed extensively with water, and characterized by carbohydrate composition, microscopy, X-ray, and solid state NMR.

2.3. Microscopies

Optic, scanning, and transmission observations were obtained as previously described.[4]

2.4. X-ray diffraction

X-ray measurements were made either on films obtained by air-drying of the suspensions of autoclaved cellulose fibers or on alkali purified fibers in a capillary tube. The X-ray diagrams were recorded as already reported.[4]

2.5. NMR spectroscopy

2.5.1. Liquid state NMR. ^{1}H and ^{13}C NMR experiments were recorded on a Bruker Avance 400 spectrometer. The sample was examined as solution in D_2O at 303 K in 5 mm o.d. tube [internal acetone: ^{1}H (CH_3) at 2.1 ppm and ^{13}C (CH_3) at 31.5 ppm relative to Me_4Si]. The inversion recovery method was used for carbon-13 $T1$ determination [two pulse sequences $(T\ldots180\ldots t\ldots90)_n$] with 12 t values ranging from 5 ms to 10 s.

2.5.2. Solid state NMR. The NMR experiments were performed on a Bruker Avance spectrometer (^{13}C frequency of 100 MHz), using proton dipolar decoupling (DD), magic angle spinning (MAS), and cross-polarization (CP). CP transfer was achieved using a ramped amplitude sequence (RAMP-CP) for an optimized total contact time of 2 ms.[23] The spinning speed was set at 6 kHz, sweep width 50,000 Hz, and recycle delay 4 s. A typical number of 10,000 scans were acquired for each spectrum. The $T1$ measurements were achieved using the pulse sequence proposed by Torchia.[24]

3. Results and discussion

3.1. Morphology

The morphology of OFI spines has already been described.[4] The body of the spine consists of a parallel arrangement of slender fibers. After alkali and chlorite treatments the fibers were still bundled together. These fibers were suspended in water, submitted to a slow mechanical stirring for 48 h, which allowed a progressive individualization of the fibers (Fig. 2A).

Each fiber had a lateral dimension of the order of 6–10 μm, an average length of 0.3–0.5 mm, and presented a small lumen. During the autoclave treatments the arabinan–polysaccharide matrix was progressively solubilized, and a bundle of cellulose microfibrils was slowly released in the medium as shown in the optical micrographs in Figure 2B and C obtained, respectively, after 1 and 3 autoclave treatments.

3.2. Alkali extraction of OFI spines

OFI spines used in this study were composed mainly of polysaccharides (96%); glucose (47.3) and arabinose (44.2%) were practically in the same amount. The spines were disencrusted by two alkaline treatments (0.5 M NaOH) for 2 h at 80 °C, and a chlorite bleaching for 2 h at 70 °C. At this stage of purification, the insoluble residue contained only carbohydrate, 50.7% of glucose, and 48.8% of arabinose (Table 1). During the alkaline extraction the pectins were solubilized, but the amount of arabinose increased.

3.3. Hydrothermal extraction of arabinan

The alkali insoluble residue consisted of fibers slightly associated with one another, composed of glucose and arabinose in the same quantities. Three successive hydrothermal treatments were performed to solubilize the arabinan component, but with only 0.125 M NaOH solution, in order to prevent at once a too large degradation of the arabinan and a conversion of cellulose I into cellulose II. The first autoclave extraction yielded 8% (arabinan **1**), the second one 10% (arabinan **2**), and the third one 8% (arabinan **3**), of the dry weight of alkali extracted residue. The three extracts were pooled together and the sugar composition revealed that they were composed mainly of arabinose (94.3%). Hereinafter, this fraction will be called arabinan.

During the alkali hydrothermal treatment, the fibers were disencrusted from the outside to the inside of the fiber, and are progressively defibrillated (Fig. 2B and C). After three hydrothermal treatments the insoluble residue still contained significant amounts (12.9%) of residual arabinose (Table 1). These data indicate that the arabinan was strongly associated with cellulose chains, and explained the fact that the microfibrils are still associated in a small bundle (Fig. 2B and C).

3.4. TFA treatment

One of the aims of this study was to preserve the original crystalline state of the cellulose, which forbids any treatment with concentrated alkali. TFA treatment at reflux was chosen, and it removed practically all the remaining arabinan as shown in Table 1. The sample contained 96.6% of glucose and only 2.8% of arabinose. At this stage the microfibrils are well individualized (Fig. 2D). This image indicates that the fibers have been completely disrupted and that the sample consists of individualized cellulose microfibrils. These microfibrils are no more than 4–6 nm in diameter. All these results confirm a strong and intimate association at a nanometric level between arabinan and cellulose microfibrils.

3.5. Chemical characterization

The composition of OFI spines was discussed above. The sugar composition of the cell wall material after the successive alkali and autoclave extractions (Table 1) showed that pectinic materials were easily solubilized, but that the arabinan–cellulose composite was difficult to dissociate. The arabinan fraction contained L-arabinose (94.3%), and traces of rhamnose (1.6%), galacturonic acid (1.4%), glucose (0.7%), and galactose (0.6%).

During the hydrothermal treatment performed at 180 °C it is very likely that some breakdown of the

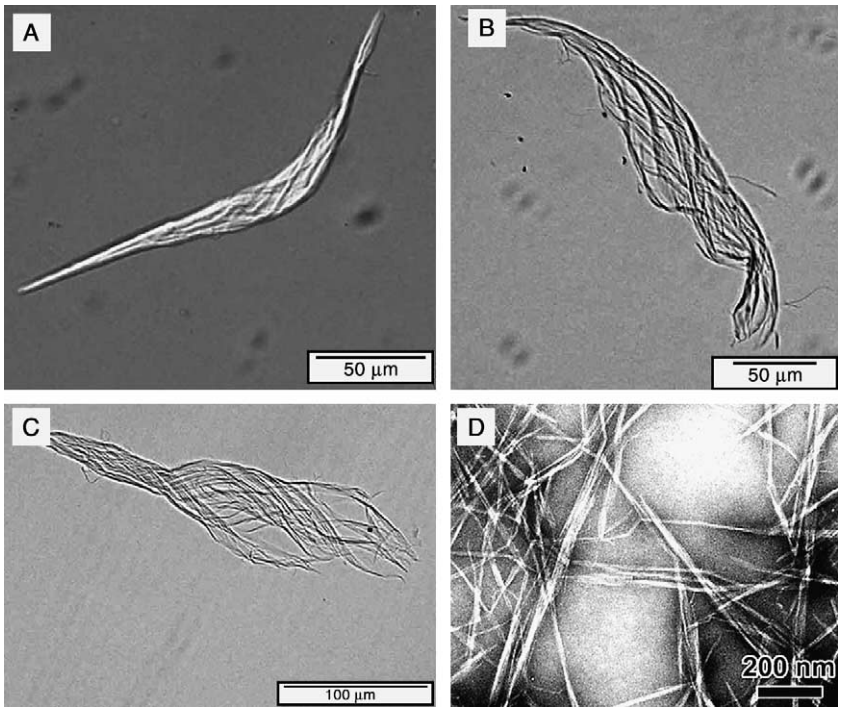

Figure 2. (A–C) Optical micrographs in Nomarski contrast of a spine fiber: (A) after alkali and bleaching, (B) as in A but after one autoclave, (C) as in A but after three autoclaves, (D) TEM photo after negative staining with uranyl acetate of spine cellulose microfibrils (as in C after TFA).

Table 1. Sugar composition[a] of OFI spines after alkali and autoclave extractions

Component	Untreated	Alkaline[b]	Autoclave **1**	Autoclave **2**	Autoclave **3**	Purified cellulose[c]
Glucose	47.3	50.7	58.6	70.6	86.5	96.6
Galactose	2.2	—	—	—	—	—
Arabinose	44.2	48.8	40.8	28.8	12.9	2.8
Rhamnose	1.1	Trace	—	—	—	—
GalA	6.3	0.5	0.6	0.3	0.2	0.6

[a] Expressed in relative weight percentages.
[b] Two alkaline extractions followed by a chlorite bleaching.
[c] As in b followed by three autoclaves and a TFA treatment.

arabinan occurred. However the arabinosyl linkage compositions of the hydrothermal extracted arabinan were similar to those found in arabinans from other plants.[5–21] We reported the results of the methylation analysis in Table 2. The overall recoveries of methylated alditol acetates were in good agreement with sugar values obtained by direct sugar analysis.

Table 2. Methylated sugars from the hydrolyzate of the methylated arabinan fraction

Sugar derivative	Molar ratios[a]	Deduced linkage
2,3,5-Me_3-Ara[b]	33.2	Terminal-Ara*f*-(1 →
2,3-Me_2-Ara	35.8	→ 5)-Ara*f*-(1 →
2-Me-Ara	14.3	→ 3,5)-Ara*f*-(1 →
3-Me-Ara	10.4	→ 2,5)-Ara*f*-(1 →
L-Arabinose	6.3	→ 2,3,5)-Ara*f*-(1 →

[a] Expressed as area percentages of the total methylated alditol derivatives.
[b] 2,3,5-Me_3-Ara = 1,4-di-*O*-acetyl-2,3,5-tri-*O*-methyl-L-arabinitol, etc.

The results suggested that the arabinan contained a (1 → 5)-arabinofuranose backbone, with 67% of the units being 1,5-linked, from which 36% were exclusively 1,5-linked. The degree of branching was around 31%, either on C-3 (14.3% of the units being 1,3,5-linked) or on C-2 (10.4% of the units being 1,2,5-linked), or both on C-2 and C-3 (6.3% of the units being 1,2,3,5-linked). On the average, 14.3 and 10.4 of the L-arabinose residues are involved in branching through C-3, C-5 and C-2, C-5, respectively, whereas 6.3 residues are branched at C-2, C-3, and C-5. The relatively high proportion of terminal sugars (33%) combined with 6.3% of arabinose units branched at C-2, C-3, and C-5, indicated that side-chain oligosaccharides have an average DP close to 1.

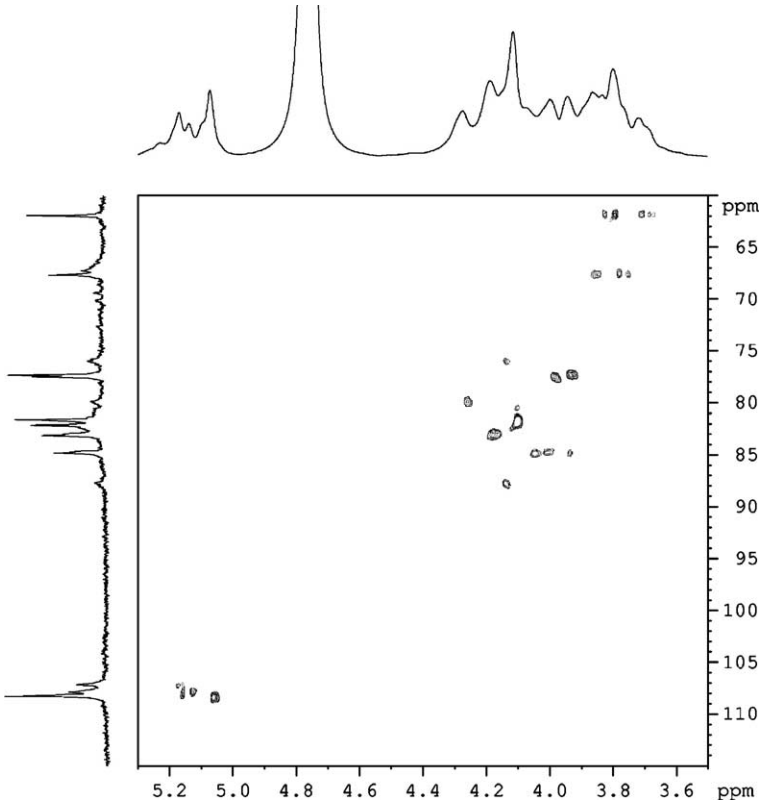

Figure 3. Contour plot of 2D heteronuclear $^{1}H/^{13}C$ shift-correlated spectrum of arabinan with 1D ^{1}H and ^{13}C spectra.

3.6. ^{1}H and ^{13}C NMR characterization

The ^{1}H and ^{13}C NMR spectra of the arabinan are shown in Figure 3. In order to facilitate the discussion, a schematic structure consistent with the methylation and NMR data is proposed in Figure 4, but many other variations are possible.

The region for anomeric proton signals in Figure 3 contains at least four signals at 5.17, 5.11, 5.08, and 5.01 ppm, with relative intensities difficult to measure as the signals are overlapping. The strong signal at 5.01 ppm was assigned to 1,5- and 1,3,5-linked α-Ara*f* (units C and E, respectively). The medium signal at 5.11 ppm corresponded to the nonreducing terminal α-Ara*f* linked to the C-2 and/or C-3 positions (unit A). The signal at 5.17 ppm can be assigned to 1,2,5- and 1,2,3,5-linked α-Ara*f* (units D and B, respectively).

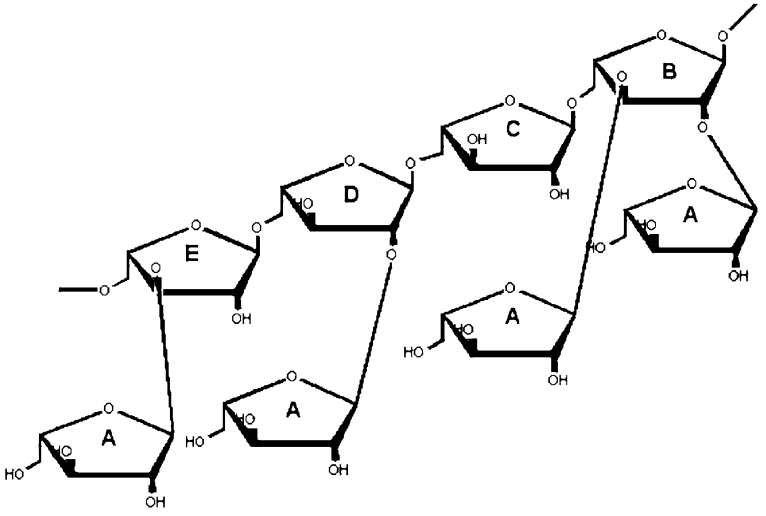

Figure 4. Schematic structure of the arabinan.

Table 3. Assignments of the ^{1}H and ^{13}C NMR spectra of the arabinan fraction (D_2O, 298 K)

Arabinosyl residues		Chemical shifts[a]				
		1	2	3	4	5
Ara-A[b]	^{1}H	5.11	4.055	3.885	4.00	3.76; 3.66
	^{13}C	107.90 (449)[c]	82.13 (388)[c]	77.33 (436)[c]	84.81(419)[c]	61.90 (241)[c]
Ara-C[b]	^{1}H	5.01	4.05	3.93	4.13	3.80; 3.73
	^{13}C	108.30 (332)	81.59 (363)	77.50 (349)	83.12 (322)	67.65 (176)
Ara-D[b]	^{1}H	5.17	4.085	4.085	4.215	
	^{13}C	107.20 (283)	—	—	—	67.65–67.20
Ara-B[b]	^{1}H	5.17	—	—	—	—
	^{13}C	107.20 (283)	87.67 (265)	75.98 (276)	79.88 (282)	67.20 (145)
Ara-E[b]	^{1}H	5.01	—	—	—	—
	^{13}C	108.30 (283)	—	—	—	67.65–67.20

[a] In ppm relative to the signal of internal acetone in D_2O, at 2.15 ppm (^{1}H) or at 31.15 ppm (^{13}C).
[b] A, B, C, D, and E units as represented in Figure 4.
[c] Carbon-13 $T1$ in millisecond appear in brackets.

The assignments of the proton signals reported in Table 3 were made according to 2D COSY experiments and literature data.[25–28] The region for signals of anomeric carbons in the ^{13}C NMR spectrum (Fig. 3) contained at least three signals at 107.20, 107.90, and 108.30 ppm with approximative relative intensities of 1, 2, 4 (small, medium, and large), respectively.

The assignments of the carbon-13 signals (Table 3) were done according to 2D hetero-correlated experiments (Fig. 3) and confirmed previous work,[6,9,13,29] but with small modifications. For instance in the HETCOR spectrum (Fig. 3), the anomeric region showed four correlations, whereas there are only three anomeric carbons in the 1D spectrum. We can observe cross-peaks between proton D-1 and carbon D-1, respectively, at 5.17 and 107.20 ppm; proton C-1 and carbon C-1, respectively, at 5.01 and 108.30 ppm; proton A-1 and carbon A-1 at 5.11 and 107.90 ppm, respectively, but also an extra cross-peak between a proton at 5.08 ppm and a carbon at 107.75 ppm. These two last correlations might arise from proton A-1 and carbon A-1 of terminal unit A but differently linked, either to the C-2 and/or C-3 positions of the backbone arabinosyl units, which explained minor upfield chemical shifts.

Carbon-13 $T1$ measurements showed that the small and broad signals, already assigned to B units branched in C-2, C-3, and C-5, have short $T1$ values of 280 ms. The residue B exhibits less segmental motion because of its location at a branch point, which makes it relax faster than the other units. Carbons of unit C in the backbone have an average $T1$ value of 350 ms, whereas carbons of unit A have longer $T1$, with an average value of 430 ms. These data are in agreement with the additional degrees of freedom provided by the terminal side-chain character of unit A. We already observed such results on molecular motion of branched-chain Klebsiella polysaccharides.[30] Carbon-13 $T1$ values of carbons 5A, 5B, and 5C of 241, 145, and 176 ms, respectively, are also in good correlation, but with values more or less divided by 2 as these carbons bear two protons.

3.7. X-ray analysis

X-ray measurements were done directly on the spine, on the individualized fibers after alkali extraction, after hydrothermal treatments, and finally after TFA hydrolysis. We observed that there is no difference in the X-ray diffraction diagrams, which showed that in the spines, the cellulose system is of substantial crystallinity and that the crystalline cellulose microfibrils were rather well aligned parallel to the spine axis. X-ray measurement on the individualized fibers, after alkali and chlorite treatments, was done in a capillary tube, in order to study the arabinan–cellulose complex under wet conditions. We observed only the cellulose diffraction patterns (Fig. 5A).

It is important to point out that after all the different chemical treatments the fibers are progressively fibrillated, but no structural modification can be observed, as the X-ray diffraction patterns showed that we still have a cellulose I crystalline structure. Indeed we already showed that primary cell wall cellulose of sugar beet is very sensitive toward aqueous alkali solutions, and mercerization started as soon as the NaOH concentration became higher than 8%.[31] In the case of cactus spine fibers, which consisted of a thin S1 primary wall and a large S2 secondary wall, we studied the influence of NaOH concentration on ultrastructural modifications. The conversion of cellulose I into cellulose II (mercerization) started when they were dispersed in aqueous NaOH at a concentration of 12% (w/w). An increase in NaOH concentration induced a progressive transformation of cellulose I into cellulose II. At a concentration of 16% the mercerization is fully complete and we have only cellulose II as observed in the X-ray diffraction pattern in Figure 5B.

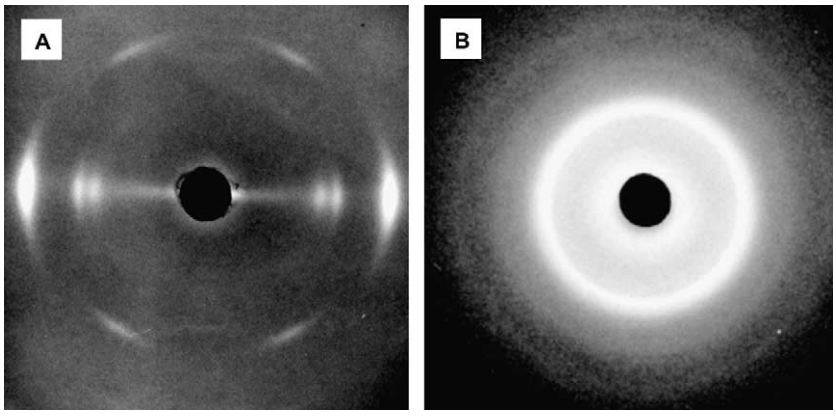

Figure 5. X-ray fiber diffraction patterns of cactus spines: (A) after alkaline and bleaching purification (capillary tube), (B) as in A but after hydrothermal extractions and treatment with 4 M NaOH.

3.8. Solid state NMR characterization

3.8.1. Composite samples. Figure 6 shows the CP-MAS NMR spectra of the spines along the purification process obtained in never-dried conditions. The raw sample spectrum (Fig. 6A) presents sharp peaks arising from the contribution of all the polysaccharides that can be found in the spine.

After NaOH and bleaching treatment (Fig. 6B) and further acidic TFA treatment (Fig. 6C), some of these resonances disappear leading to a typical native cellulose I spectrum already observed for several specimens. The close inspection of these differences, combined with the sugar analysis and liquid state NMR on solubilized fractions allows us to propose an assignment of all the peaks presented in Table 4. However, due to the intrinsic lower resolution of solid state NMR as compared to liquid state, we were not able to distinguish between all the arabinose carbons. It should nevertheless be noticed that native cellulose does not display any peak above 105.7 ppm. This spectral feature allows us to evidence three different groups of anomeric carbon clearly seen in the bleached sample spectrum at 107.9, 107.4, and 106.6 ppm (Fig. 6B), which can be can be favorably compared to the liquid state NMR assignment of the arabinose residues presented in Table 3.

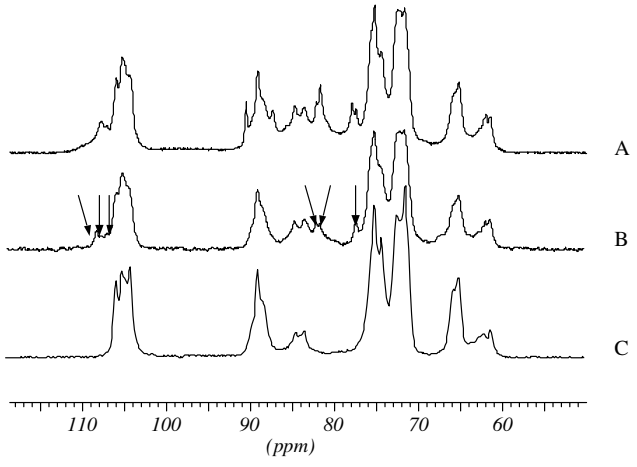

Figure 6. CP-MAS ^{13}C NMR spectra of never-dried cactus spines: (A) original, (B) after alkaline and bleaching treatments, (C) as in B but after acidic TFA treatment. Arrows indicate the presence of isolated arabinan signals.

This spectral separation between arabinan and cellulose signal allows us to estimate the relative amount of each polysaccharide to the overall spectra. One has to remember beforehand that in the CP-MAS Hartman–Hahn conditions, only the signals arising from rigid molecular moieties, that is, with motion correlation times much longer than tens of a microsecond are quantitatively polarized. Direct signals from moieties in the liquid state do not appear in the CP-MAS spectra. We measured an approximate amount of solid-like arabinan of 20%, far from the equal repartition (50:50) of both components as shown by the sugar analysis. This clearly indicates that the arabinan part of the composite in hydrated conditions is submitted to high rate molecular motions. However, the presence of measurable signals at 107.9, 107.4, and 106.6 ppm proves that a part of the arabinan is in strong interaction with the cellulose. In the absence of such an interaction no signal would have been detected.

To go further in the understanding of the dynamic of the composite, we measured the $T1$ of the carbons in the bleached sample (Table 4). The peaks that can be attributed to cellulose alone clearly exhibit very long relaxation times, 36.9 s (C1-Iβ), 30 s (C1-Iα), and 58.5 s (C4-Iα + Iβ), in agreement with the highly crystalline nature of cellulose. It can be noticed that carbons of the amorphous cellulose part have shorter $T1$ values (11.9 and 12.7 s in the case of C4). More interestingly, the peaks arising from the arabinan alone show a two relaxation times behavior, with longer times corresponding to moieties with hindered motions (5.6 s for C1-A, 8.8 and 12.5 s for C2-A), and shorter times arising from

Table 4. Chemical shift, assignment, and $T1$ values of C1 and C4 carbons in the bleached spines

δ (ppm)	107.9	107.4	106.6	105.7	104.9	88.8	84.5	84.3	81.9	81.4
Assignment	C1-A[a]	C1-A[a]	C1-A[a]	C1-Iβ[b]	C1-Iα[b]	C4-(Iα + β)[b]	C4-Cam[c]	C4-Cam[c]	C2-A[a]	C2-A[a]
$T1$ (s)	ND[d]	ND[d]	0.9 (67%) 5.6 (33%)	36.9	30	58.5	12.7	11.9	0.9 (70%) 8.8 (30%)	0.8 (63%) 12.5 (37%)

[a] A: arabinan.
[b] Iβ, Iα, Iα + Iβ: crystalline part of the cellulose.
[c] Cam: amorphous part of the cellulose.
[d] ND: due to their poor sensibility, $T1$ values of these peaks have not been determined.

more mobile fragments (0.9 s for C1-A and C2-A, 0.8 s for C2-A). The amount of this strongly immobilized part of the arabinan can be estimated roughly at 33%. The relatively good resolution of the peaks attributed to the arabinan components is then clearly due to their fast molecular motions. From this, it can be very roughly estimated that around 15% of the arabinan is in strong interaction having a solid-like behavior, whereas 25% undergoes hindered motions, and 60% is in a liquid-like state.

The samples without water after freeze drying were also investigated. Figure 7 shows the comparison between the spectra obtained for original and purified samples. The purified cellulose spectrum (Fig. 7B) is typical of dried cellulose, with changes in the resolution of the peaks arising from the disordered cellulose chains on the surface of the crystal. The spectrum of the original spines (Fig. 7A) shows a dramatic increase of the line widths of the peaks attributed to the arabinan component. These wide signals can be related to the amorphous character of this hemicellulosic part of the composite and to the quenching of the molecular motion. In the light of the $T1$ measurements previously discussed, it can be deduced that water enhances the molecular motions of the arabinan. Moreover, a quantitative evaluation of the arabinan content gives a value of 45%, very close to the data measured by sugar analysis. These observations confirm that the arabinan–cellulose composite consists of cellulose microfibrils in strong interaction with a swollen but stiff arabinan gel.

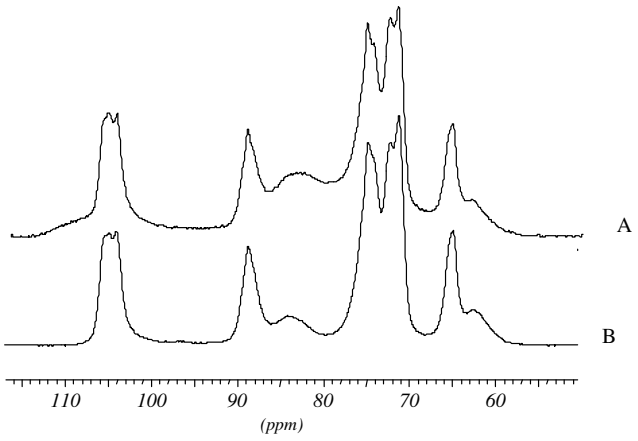

Figure 7. CP-MAS ^{13}C NMR spectra of freeze-dried cactus spines: (A) original, (B) after alkaline and bleaching treatments.

3.8.2. Purified cellulose samples. The CP-MAS spectrum of the purified cellulose allows us to evaluate both the ratio between the Iα and Iβ allomorphs and the crystallinity index of the cellulose microfibrils. The precise deconvolution, as described,[32] of the purified cellulose spectrum gives a Iβ content of 85% (±2%), whereas the crystallinity index was evaluated at 0.70 (±0.02). These spectral features indicate that the present samples have a crystallinity comparable to that of cotton.[33] Both the high Iβ content and high crystallinity index indicate that the cellulose of these spines can be classified in the category of highly ordered microfibrils of secondary walls. Thus they show superior properties to those of wood fibers.[34] From our NMR data, it is also possible to evaluate the lateral size of the microfibrils. Indeed, with a crystallinity index of 0.70, this lateral size can be estimated to be around 6 nm.

4. Conclusion

The spines of OFI prickly pear cactus consist of a compact parallel arrangement of fibers, composed mainly of two polysaccharides, cellulose and arabinan, practically in equal amounts. The NMR experiments are in good agreement with the chemical data, and confirmed that the arabinan is moderately branched, with 67 α-L-arabinofuranose residues (1 → 5)-linked in the backbone, and 33 units as terminal side chains. The degree of branching was around 31%, either on C-3 or C-2, or both on C-2 and C-3. The presence of this arabinan is also confirmed by CP-MAS solid state NMR. Moreover, the dynamical properties of the arabinan moiety indicate that one part of it is in the form of stiff a swollen gel, the other part being in strong interaction with cellulose microfibrils.

From a morphological point of view, X-ray analysis confirms that the cellulose in OFI spine fibers is of high crystallinity, with microfibrils aligned parallel to the spine axis. As far as we know, the OFI spine fibers are

a unique example of a practically perfect 50:50 arabinan–cellulose natural composite without any other hemicellulosic components. To our knowledge, our study reports for the first time arabinan in strong interaction with cellulose microfibrils inside secondary wall fibers. This particular association, together with the aforementioned high degree of alignment is probably responsible for the very high mechanical properties of the OFI spines. Future research will focus on a further elucidation of this very original arabinan–cellulose (1:1) complex composite, particularly on the mutual arrangement of the arabinan and cellulose microfibrils inside the spine fibers.

Acknowledgements

The authors acknowledge the financial help of the Rhône Alpes region (TEMPRA Sud-Méditerranée) and the Comité Mixte Franco-Marocain (AI 236/SVS/00). They thank Dr. C. Fraschini, Mrs. D. Dupeyre, and Dr. J.-L. Putaux for their help in NMR, SEM, and TEM.

References

1. Nobel, P. S.; Garcia-Moya, E.; Quero, E. *Plant Cell Environ.* **1992**, *15*, 329–335.
2. Park, E. H.; Kahng, J. H.; Paek, E. A. *Arch. Pharmacal. Res.* **1998**, *21*(1), 30–34.
3. Medellin, M. L. C.; Salvidar, S. O. S.; De la Garza, J. V. *Arch. Latinoam. Nutri.* **1998**, *48*(4), 316–323.
4. Malainine, M. E.; Dufresne, A.; Dupeyre, D.; Mahrouz, M.; Vuong, R.; Vignon, M. R. *Carbohydr. Polym.* **2003**, *51*, 77–83.
5. Joseleau, J.-P.; Chambat, G.; Lanvers, M. *Carbohydr. Res.* **1977**, *122*, 107–113.
6. Capek, P.; Toman, R.; Kardosova, A.; Rosik, J. *Carbohydr. Res.* **1983**, *117*, 133–140.
7. Siddiqui, I. R.; Emery, J. P. *J. Agric. Food Chem.* **1990**, *38*(2), 387–389.
8. Karacsonyi, S.; Toman, R.; Janecek, F.; Kubackova, M. *Carbohydr. Res.* **1975**, *44*, 285–290.
9. Joseleau, J.-P.; Chambat, G.; Vignon, M. R.; Barnoud, F. *Carbohydr. Res.* **1977**, *58*, 165–175.
10. Roudier, A. J.; Eberhard, L. *Bull. Soc. Chim. Fr.* **1965**, *2*, 460–464.
11. Jiang, K. S.; Timell, T. E. *Cellul. Chem. Technol.* **1972**, *6*, 499–502.
12. Swamy, N. R.; Salimath, P. V. *Phytochemistry* **1991**, *30*, 263–265.
13. Eriksson, I.; Andersson, R.; Westerlund, E.; Aman, P. *Carbohydr. Res.* **1996**, *281*, 161–172.
14. Zawadzki-Baggio, S. F.; Sierakowski, M.-R.; Corrêa, J. B. C.; Reicher, F. *Carbohydr. Res.* **1992**, *233*, 265–269.
15. Churms, S. C.; Merrifield, E. H.; Stephen, A. M.; Walwyn, D. R.; Polson, A.; van der Merwe, K. J.; Spies, H. S. C.; Costa, N. *Carbohydr. Res.* **1983**, *113*, 339–344.
16. Guillon, F.; Thibault, J.-F. *Carbohydr. Res.* **1989**, *190*, 85–96.
17. Guillon, F.; Thibault, J.-F.; Rombouts, F. M.; Voragen, A. G. J.; Pilnik, W. *Carbohydr. Res.* **1989**, *190*, 97–108.
18. Oosterveld, A.; Beldman, G.; Schols, H. A.; Voragen, A. G. *Carbohydr. Res.* **1996**, *288*, 143–153.
19. McNeil, M.; Darvill, A. G.; Albersheim, P. The Structural Polymers of the Primary Cell Walls of Dicots. In *Progress in the Chemistry of Organic Natural Products*; Herz, W., Grisebach, H., Kirby, G. W., Eds.; Springer: Vienna, 1979; Vol. 37, pp 191–249.
20. Davis, E. A.; Derouet, C.; Hervé du Penhoat, C.; Morvan, C. *Carbohydr. Res.* **1990**, *197*, 205–215.
21. Vignon, M. R.; Garcia-Jaldon, C. *Carbohydr. Res.* **1996**, *296*, 249–260.
22. Sanford, P. A.; Conrad, H. E. *Biochemistry* **1966**, *5*, 1508–1517.
23. Peersen, O. B.; Wu, X.; Kustanovich, I.; Smith, S. O. *J. Mag. Res. A* **1993**, *104*, 334–339.
24. Torchia, D. A. *J. Mag. Res.* **1978**, *30*, 613–616.
25. Hervé du Penhoat, C.; Michon, V.; Goldberg, R. *Carbohydr. Res.* **1987**, *165*, 31–42.
26. Saulnier, L.; Brillouet, J.; Moutounet, M.; Hervé du Penhoat, C.; Michon, V. *Carbohydr. Res.* **1992**, *224*, 219–235.
27. Dong, Q.; Fang, J.-N. *Carbohydr. Res.* **2001**, *332*, 109–114.
28. Navarro, D. A.; Cerezot, A. S.; Stortz, C. A. *Carbohydr. Res.* **2002**, *337*, 255–263.
29. Backinovskii, L. V.; Nepogod'ev, S. A.; Kotchetkov, N. K. *Carbohydr. Res.* **1985**, *137*, C1–C3.
30. Vignon, M. R.; Michon, F.; Joseleau, J. P.; Bock, K. *Macromolecules* **1983**, *16*, 835–838.
31. Dinand, E.; Vignon, M. R.; Chanzy, H.; Heux, L. *Cellulose* **2002**, *9*, 7–18.
32. Heux, L.; Dinand, E.; Vignon, M. R. *Carbohydr. Polym.* **1999**, *40*, 115–124.
33. Hirai, A.; Horii, F.; Kitamaru, R. *J. Polym. Sci., Part C: Polym. Lett.* **1990**, *23*(11), 357–361.
34. Hult, E. L.; Larsson, P. T.; Iversen, T. *Cellulose* **2000**, *7*, 35–55.